

Research Paper

Modelling the Acoustic Properties of Baffles Made of Porous and Fibrous Materials

Krzysztof KOSAŁA

*Faculty of Mechanical Engineering and Robotics, Department of Mechanics and Vibroacoustics
AGH University of Krakow*Kraków, Poland; e-mail: kosala@agh.edu.pl*(received February 24, 2023; accepted January 21, 2024; published online April 12, 2024)*

The research described in the article addresses the problem of measurement, prediction and practical use of the acoustic properties of materials determined in an impedance tube. The aim of the research was to develop a simple calculation model for the insertion loss of small machinery enclosures, based on the normal incidence sound transmission loss and the normal incidence sound absorption coefficient of porous and fibrous materials. Both experimental and model tests were carried out on materials such as mineral wool, melamine foam and rebonded polyurethane foam.

Assessing the absorption properties of the tested porous and fibrous materials was performed using selected theoretical models, relating the calculations of the normal incidence sound absorption coefficient to measurements of this parameter conducted using an impedance tube. The application of the modified Allard and Champoux model brought the best results with the smallest discrepancies of the obtained results in relation to the experimental tests.

Assessing the sound-insulating properties of the tested mineral wool was carried out using the proposed calculation model for the normal incidence sound transmission loss, relating the obtained results to measurements conducted using an impedance tube. The assessment of the sound-insulating properties of porous and fibrous materials was performed using the proposed calculation model for insertion loss, which was validated using two prototype test stands for determining the insertion loss of cubic enclosures, in this case with walls made of porous and fibrous materials. Satisfactory results were obtained for engineering applications in the calculation results using the proposed models with respect to measurements. The results may have practical applications in assessing the effectiveness of acoustic enclosures, in which the basic construction material is an appropriate porous or fibrous plate, selected to have both sound-absorbing and sound-insulating properties.

Keywords: sound absorption coefficient; insertion loss; sound transmission loss; acoustical enclosures; porous materials.



Copyright © 2024 The Author(s).
This work is licensed under the Creative Commons Attribution 4.0 International CC BY 4.0
(<https://creativecommons.org/licenses/by/4.0/>).

Acronyms

α – random incidence sound absorption coefficient,
 α_f – normal incidence sound absorption coefficient,
 f – frequency,
 h – specimen thickness,
IL – insertion loss,
 m_p – surface density,
nTL – normal incidence sound transmission loss,
PCC – Pearson’s linear correlation coefficient,
 r – airflow resistivity,
 R – sound reduction index,
RMSE – root mean square error,
 R_S – airflow resistance.

1. Introduction

In issues related to the construction of anti-noise protection, such as acoustic barriers, enclosures or shields of noisy sound sources, both materials resistant to the penetration of sound waves and absorbing sound energy are used (ENGEL, SIKORA, 1997; FIEBIG, DĄBROWSKI, 2020; MORZYŃSKI, SZCZEPAŃSKI, 2018; VER, BERANEK, 2006). The basic acoustic parameter determining the properties of sound-insulating or sound-absorbing and insulating baffles, from which these protections are constructed, is the sound insulation.

Porous and fibrous materials are used in anti-noise protection, mainly as cores or sound-absorbing linings

in the construction of sound-absorbing and insulating baffles. The use of single materials, such as felt, can be found, among others, in the screening of office spaces at workstations in open-space rooms. Usually, the study of the acoustic properties of porous and fibrous materials consists of determining the sound absorption coefficient for the case of a sound wave incident perpendicularly on the specimen, which takes place during preliminary tests, especially for new materials, or for the random incidence of the sound wave on a specimen of relatively large size. Less frequently, studies are conducted to determine the extent to which these materials are resistant to sound wave penetration. The effectiveness of porous and fibrous materials in this respect is associated with increased density, and thus the airflow resistance, and with their appropriately large thickness, when insulation for lower frequency bands is desired.

The normal incidence sound absorption coefficient (α_f) of porous and fibrous materials can be determined using the semi-phenomenological and macroscopic empirical calculation models (COX, D'ANTONIO, 2017). Modelling sound propagation using a semi-phenomenological approach is more complicated and harder to use than an empirical one. Calculation of the characteristic impedance and propagation wavenumber requires knowledge of many material properties, such as porosity, airflow resistivity, tortuosity, viscous and thermal characteristic lengths, which are obtained by considering the microscopic propagation within the pores. An example of the semi-phenomenological approach is the model developed by ALLARD and CHAMPOUX (1992). The best-known empirical models include the model developed by DELANY and BAZLEY (1970) and models of other researchers such as MIKI (1990), MECHEL (1988), and QUNLI (1988). In these models, the impedance and wavenumber were determined empirically. To predict the absorption of sound-absorbing materials using these models, it is necessary to know the specific airflow resistivity and material thickness.

Research on materials of the porous and fibrous structures, used as linings or sound-absorbing cores in baffles, generally focuses on determining their absorbing properties. The problems of sound insulation properties of such materials are also investigated, although on a smaller scale (BIES, HANSEN, 2009). Sound insulation and sound absorption parameters of materials and baffles are determined primarily by laboratory tests (BATKO *et al.*, 2017; BERARDI, IANNACE, 2015; NURZYŃSKI, 2022; PUTRA *et al.*, 2015), while, with material data, they can also be estimated using calculation models (DAVY, 2009; SHARP, 1973; TRINH *et al.*, 2022; KOSAŁA *et al.*, 2020a).

The article focuses on the research into a certain group of sound-absorbing materials in the form of plates, which also have sound-insulating properties, especially when they are high-density materials, above

100 kg/m³, and with a large thickness of at least 50 mm.

While increasing the thickness of porous and fibrous materials, better absorption towards lower frequencies is obtained. An increase in the density of the material causes a decrease in the maximum absorption, which for this type of material occurs in higher frequency bands, and an increase in absorption in the region of lower frequencies, for which the sound absorption coefficient is generally low.

The sound insulation of baffles is defined by the sound reduction index R (International Organization for Standardization [ISO], 2021), which is determined in laboratory conditions, with the specimen placed in the measurement window separating coupled reverberation, transmitting and receiving rooms.

The sound reduction index R (also known as the sound transmission loss, TL) is defined as:

$$R = 10 \log_{10} \left(\frac{1}{\tau} \right) = 10 \log_{10} \left(\frac{W_i}{W_t} \right), \quad (1)$$

where τ is the transmission coefficient defined by the sound power, the ratio of the transmitted power W_t and the power W_i incident on the specimen.

For laboratory measurement using sound pressure, R is calculated from the equation:

$$R = L_1 - L_2 + 10 \log_{10} \left(\frac{S}{A} \right), \quad (2)$$

where L_1 and L_2 are the average energy sound pressure level in dB in the source and receiving room, respectively, S is the area in m² of the free test opening in which the specimen is installed, and A is the equivalent sound absorption area in the receiving room, also in m².

It is assumed that the sound fields are diffuse and that only sound radiated into the receiving room is from the specimen.

The parameter insertion loss (IL) is used to determine the effectiveness of acoustic enclosures, as the difference between the sound power levels of the unenclosed and enclosed sound sources (VER, BERANEK, 2006), according to the formula,

$$IL = 10 \log \left(\frac{W_0}{W_E} \right) = L_{W0} - L_{WE}, \quad (3)$$

where W_0 and W_E are the sound power radiated by the unenclosed and enclosed sources, respectively, while L_{W0} and L_{WE} are the corresponding sound power levels.

Laboratory methods for the determination of IL of small machine enclosures are specified in (ISO, 2009). Evaluating the IL of acoustic enclosures with lined slits, using this standard, is shown in one work (NIE-RADKA, DOBRUCKI, 2018). Research on the properties of sound-insulating and sound-absorbing and insulating enclosures using a prototype test stand developed for this purpose is shown in some works (KOSAŁA *et al.*, 2020b; KOSAŁA, 2022).

In the case of porous or fibrous structures, the sound insulation properties of such materials, for conditions in which the sound wave falls perpendicularly on the specimen, can be determined using an impedance tube (JIANG *et al.*, 2017; KUNIO *et al.*, 2009; KOSALA, 2021), determining the normal incidence sound transmission loss parameter (nTL) (ASTM E2611-19, 2019), which is defined as ten times the common logarithm of the normal incidence sound transmission coefficient's reciprocal.

Two different parameters, nTL and R , cannot be compared with each other because they concern the normal or random incidence of sound on the specimen, respectively. Currently, there are no known methods to determine the correlation between these parameters. The method of determining nTL is used to compare the insulating properties of small specimens.

The purpose of the research described in the article is to determine the acoustic properties of single baffles made of porous and fibrous materials, which relate to the absorption and resistance of these materials to sound penetration. Acoustic tests were carried out using an impedance tube and two prototype stands for determining the IL of cubic enclosures, in this case with walls made of porous and fibrous materials.

Calculation models for the nTL of mineral wools and for the IL of an acoustic enclosure in the form of a cube using plates with the porous and fibrous structures were proposed. The calculation model for the IL for porous and fibrous materials can be used when their basic acoustic parameters in the form of the α_f and the nTL are known. For baffles made of fibrous materials, in the form of mineral wool, material data, including airflow resistance, is sufficient to determine the IL of the enclosure. Validation of the calculation models was carried out using two developed prototype stands for determining the acoustic properties of enclosures.

2. Specimens' material data

Three high-density materials, above 100 kg/m^3 , were tested, i.e., mineral wool and rebonded polyurethane foam, and a material with very low density and high absorption, i.e., melamine foam. All materials had comparable thicknesses of 50 mm or 60 mm. Figure 1 shows specimens of materials whose round shape resulted from the tests carried out on them, which were tests of air flow resistance (discs with a diameter of

100 mm) and the α_f and the nTL (discs with a diameter of 34.9 mm).

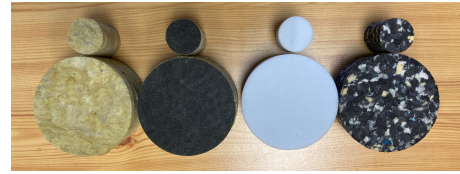


Fig. 1. Material specimens of mineral wool (MW151), mineral wool with glass fleece (MW100), melamine foam (ME), and rebonded polyurethane foam (PU).

Table 1 shows the material data of the specimens made of the same materials as shown in Fig. 1, but in the form of plates, whose square shape was associated with their use as walls of acoustic enclosures in the shape of cubes with wall dimensions of $0.55 \text{ m} \times 0.55 \text{ m} \times 0.55 \text{ m}$ and $0.7 \text{ m} \times 0.7 \text{ m} \times 0.7 \text{ m}$.

3. Testing methods and test facilities

3.1. The airflow resistance

In order to determine the airflow resistance of materials R_S (ISO, 2020), the Norsonic Nor1517A stand was used, which is the equipment of the laboratory for testing the acoustic properties of materials and structures at the Department of Mechanics and Vibroacoustics of the AGH University of Science and Technology. The tests were carried out using alternating airflow methods (ISO, 2020), using material specimens with a diameter of 100 mm, as shown in Fig. 1. The measurements of the R_S , were carried out for the atmospheric conditions prevailing in the laboratory, i.e., at a temperature of $22 \text{ }^\circ\text{C}$ and an atmospheric pressure of 1002 hPa.

Due to the fact that the theoretical calculation models for the α_f , used in further sections of the article, do not use the R_S values obtained directly from the measurements, but the airflow resistivity, the values of this parameter were also calculated. The airflow resistivity (r) is defined as the airflow resistance (R_S) per unit length, which is the specimen thickness (h):

$$r = \frac{R_S}{h}. \quad (4)$$

The obtained values of R_S and r for the four analysed materials are shown in Table 1.

Table 1. Specimens' material data.

ID	Material	Density [kg/m^3]	The size of the side of a square plate [m]	Plate thickness (h) [m]	The airflow resistance (R_S) [$\text{Pa} \cdot \text{s} \cdot \text{m}^{-1}$]	The airflow resistivity (r) [$\text{Pa} \cdot \text{s} \cdot \text{m}^{-2}$]
MW151	Mineral wool	151.4	0.55	0.06	6417.8	106963.3
MW100	Mineral wool with glass fleece	100.2	0.7	0.05	1811.0	36220.8
ME	Melamine foam	9	0.7	0.05	669.2	13384.8
PU	Rebonded polyurethane foam	214.4	0.55	0.05	2394	47880

3.2. Normal incidence sound absorption coefficient and the normal incidence sound transmission loss

The experimental tests were carried out in the laboratory for testing the acoustic properties of materials and structures, in accordance with the relevant standards: (ISO, 2001) for the α_f , and (ASTM E2611-19, 2019) for the nTL. Both parameters were determined using a Mecanum Inc. impedance tube, which enabled the determination of the values of these parameters in the lower and higher frequency ranges for material specimens of one diameter, 34.9 mm. The measuring apparatus was identical to the tests described in (KOSAŁA, 2021).

The specificity of the laboratory stand used, with a Mecanum Inc. impedance tube, the Siemens LMS SCADAS Mobile analyzer, a computer with Simcenter Testlab software, and type 378A14 PCB measuring microphones, spaced 65 mm or 29 mm apart, respectively, for the low and high frequency ranges, allowed the acoustic parameters to be determined, after averaging the results, in the range of 50 Hz to 5700 Hz.

3.3. Insertion loss of enclosure

In the Department of Mechanics and Vibroacoustics, a prototype stand for testing the acoustic properties of baffles and enclosures was developed (KOSAŁA *et al.*, 2020b). So far, single rigid homogeneous baffles of various thicknesses (steel, aluminium, plastics) have been tested on this stand, which, together with an omnidirectional sound source placed inside, imitating a noisy machine or device, constituted a sound-insulating enclosure (KOSAŁA *et al.*, 2020b; KOSAŁA, 2022), as well as two-layer baffles made of a rigid plate and a layer of material in the form of mineral wool, constituting the sound-absorbing and insulating enclosure. This stand allows baffles with a thickness of 1 mm to 90 mm and external dimensions of 0.7 m \times 0.7 m to be tested.

Another developed stand, also consisting of a steel frame, enables the testing of baffles with the same thickness range, but with external dimensions of 0.55 m \times 0.55 m. The construction of the new stand for testing baffles and enclosures is schematically shown in Fig. 2. Five identical baffles form an acoustic enclosure. As in the case of the former enclosure, an omnidirectional sound source placed centrally was used for acoustic tests (Fig. 2).

The walls of the enclosure are pressed against the steel frame using mechanisms and clamping frames, similarly to the solution described in detail in some works (KOSAŁA *et al.*, 2020b; KOSAŁA, 2022), as shown in Fig. 3, where material made of rebonded polyurethane foam (PU) was used as the walls of the enclosure.

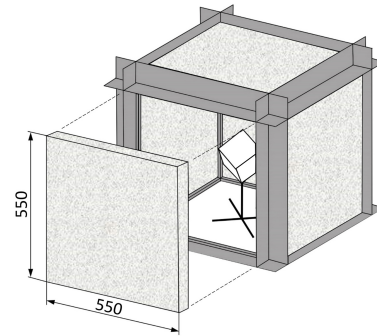


Fig. 2. The scheme of the enclosure frame with a sound source and five walls.

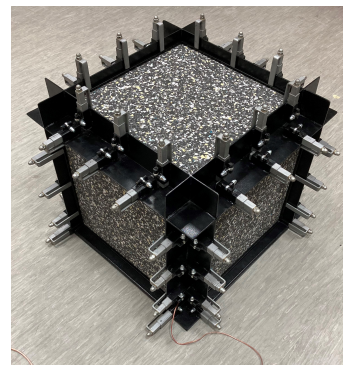


Fig. 3. Enclosure with walls made of PU boards with dimensions of 0.55 m \times 0.55 m \times 0.05 m.

To test the acoustic properties of single homogeneous materials – plates made of porous and fibrous materials, both stands were used, designed for walls with dimensions of 0.7 m \times 0.7 m and 0.55 m \times 0.55 m. The purpose of using these two stands was to check whether, using the theoretical computational models described in the article, it is possible to estimate the spectral characteristics of ILs, taking into account enclosures of different dimensions.

In order to determine the effectiveness of an acoustic enclosure built of five identical walls for the four tested materials, the IL of the enclosure was determined using Eq. (3). The tests of the sound power level were carried out in the measurement conditions and with the use of measurement equipment identical to those described in (KOSAŁA, 2022). The sound power levels were determined in a room with a capacity of 79 m³, using the survey method in accordance with the standard (ISO, 2010).

4. Results of experimental tests

4.1. Normal incidence sound absorption coefficient and the normal incidence sound transmission loss

Due to the fact that the frequency range for the IL of the acoustic enclosure made of the tested materials

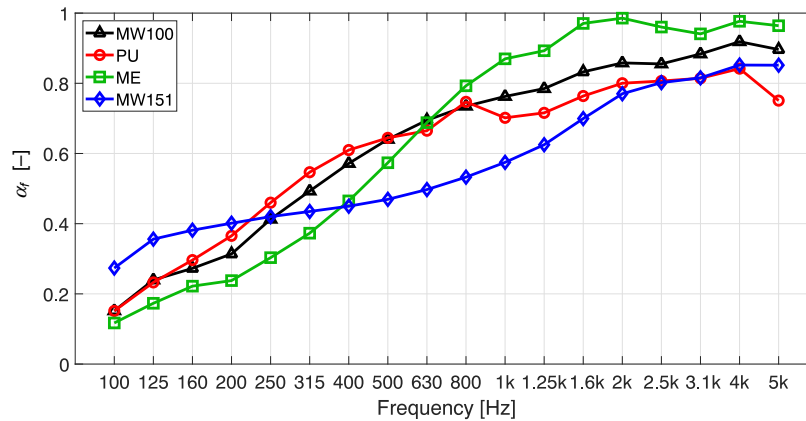


Fig. 4. Normal incidence sound absorption coefficient (α_f) of materials: MW100, PU, ME, and MW151.

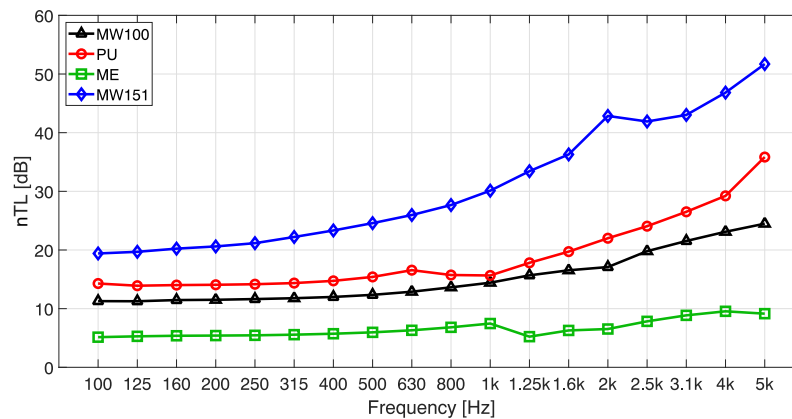


Fig. 5. Normal incidence sound transmission loss (nTL) of materials: MW100, PU, ME, and MW151.

was 100 Hz to 5000 Hz, the values of the α_f and the nTL were also presented in the $1/3$ octave frequency bands for the same frequency range as shown in Figs. 4 and 5, respectively.

The highest values of the nTL, amounting to 0.8–0.98, were found in the material with the lowest density (9 kg/m^3), which was the melamine foam for the frequency range from 800 kHz to 5 kHz (Fig. 4). The mineral wool with the highest density, MW151, had the lowest values of the absorption coefficient among the tested materials, but it was the best at absorbing sounds for low frequencies, 100 Hz to 200 Hz. Usually, increased absorption in the lower frequency range, at the cost of decreased absorption in the higher frequency range, is obtained when the airflow resistivity is too high. For this reason, for mineral wool with the highest airflow resistivity ($r = 106.9 \text{ kPa} \cdot \text{s} \cdot \text{m}^{-2}$), MW151, the shape of the spectral characteristics of the α_f differs significantly from the characteristics of other materials, as shown in Fig. 4.

As expected, the material with the lowest density (ME) showed the lowest values of the nTL, which for the $1/3$ octave frequency bands do not exceed 10 dB (Fig. 5). With the increase in frequency, the increase in the nTL for the ME specimen was the smallest

among the tested materials. The tests showed that mineral wool with a density of 151 kg/m^3 had the best resistance to sound penetration with the perpendicular sound wave incidence on the specimen. The rebonded polyurethane foam with a much higher density (214 kg/m^3) had weaker sound insulation properties compared to this mineral wool, depending on the frequency of values, by about 5 dB to 15 dB. It should be taken into account here that the rebonded polyurethane foam is a less homogeneous material than wool.

4.2. Insertion loss of the enclosure

Figures 6 and 7 show spectral characteristics of the IL in $1/3$ octave frequency bands for materials in the form of baffles with dimensions of $0.7 \text{ m} \times 0.7 \text{ m}$, which were MW100 and ME, and baffles with dimensions of $0.55 \text{ m} \times 0.55 \text{ m}$, which were MW151 and PU.

Comparing the IL of the enclosure with walls made of MW100 and ME plates, dimensions $0.7 \text{ m} \times 0.7 \text{ m}$ (Fig. 6), it can be seen that the differences are on average about 6 dB, for frequencies lower than 800 Hz, and the range from 4 dB to 8 dB for a given centre frequency of the $1/3$ octave band. Above a frequency of 800 Hz, the IL difference increases with frequency from

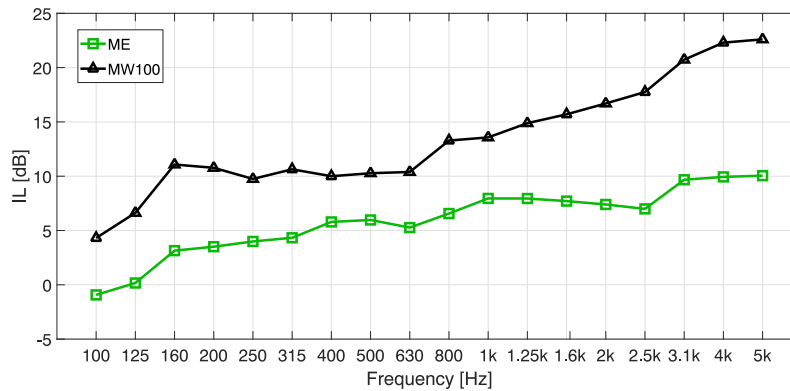


Fig. 6. Insertion loss (IL) of an acoustic enclosure with walls measuring 0.7 m \times 0.7 m made of MW100 and ME materials.

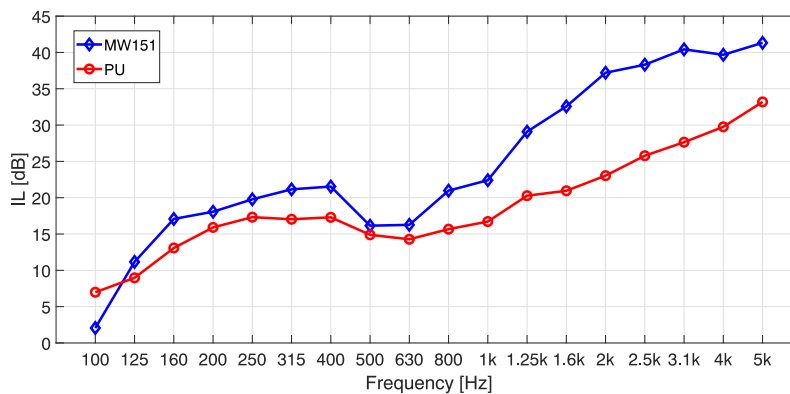


Fig. 7. Insertion loss (IL) of an acoustic enclosure with walls measuring 0.55 m \times 0.55 m made of MW151 and PU materials.

5.6 dB up to 12.5 dB. The average value of the difference for this frequency range is 9.5 dB.

In Fig. 7, which concerns IL for an enclosure with smaller wall dimensions (0.55 m \times 0.55 m), made of MW151 and PU plates, the curve of this parameter has a shape with a visible reduction in the IL value for the frequency of 630 Hz. The reason for this phenomenon may be the resonance of the enclosure cavity, whose impact on the spectral characteristics of IL is much more visible when we are dealing with rigid plates constituting the walls of the sound-insulating enclosures, which was considered in a previous work (KOSAŁA, 2022). The shape of the spectral characteristics shown in Fig. 7 may be influenced by a certain stiffness of the enclosure walls, which causes the tested porous and fibrous materials (PU and MW151) to behave like stiff plates. It can be assumed that the nature of the IL curves for MW151 and PU materials (Fig. 7) is similar only in the frequency range from 100 Hz to 630 Hz. In this frequency range, the differences in IL values for individual centre frequencies are relatively small and average about 3 dB, with a range from about 1 dB to 5 dB. A significantly higher IL value for the MW151 mineral wool compared to the rebounded polyurethane foam PU can be observed above the frequency of 630 Hz. With the exception of the centre frequencies of 4 kHz and 5 kHz, as the frequency

increases, the IL of the MW151 mineral wool also increases, on average by about 10 dB, oscillating from a difference of about 5 dB to about 14 dB.

5. Modelling of acoustic properties of porous and fibrous materials

5.1. Calculation models of the normal incidence sound absorption coefficient for porous and fibrous materials

As part of the research described in this article, it was checked which of the empirical models such as Qunli, Mechel, Miki, and Delany and Bazley, is best suited for the prediction of the tested porous and fibrous materials. In addition, the Allard and Champoux model, modified by OLIVA and HONGISTO (2013) was also used. This model, among the eight empirical ones tested in (OLIVA, HONGISTO, 2013), achieved the best prediction accuracy, determined by comparing the predicted and measured absorption coefficients of 82 mineral wool configurations.

The results of calculations of the α_f using empirical models in relation to the results of laboratory tests, described in Subsec. 3.2, are shown in Fig. 8.

In order to determine the discrepancies between the calculations using the models and the results ob-

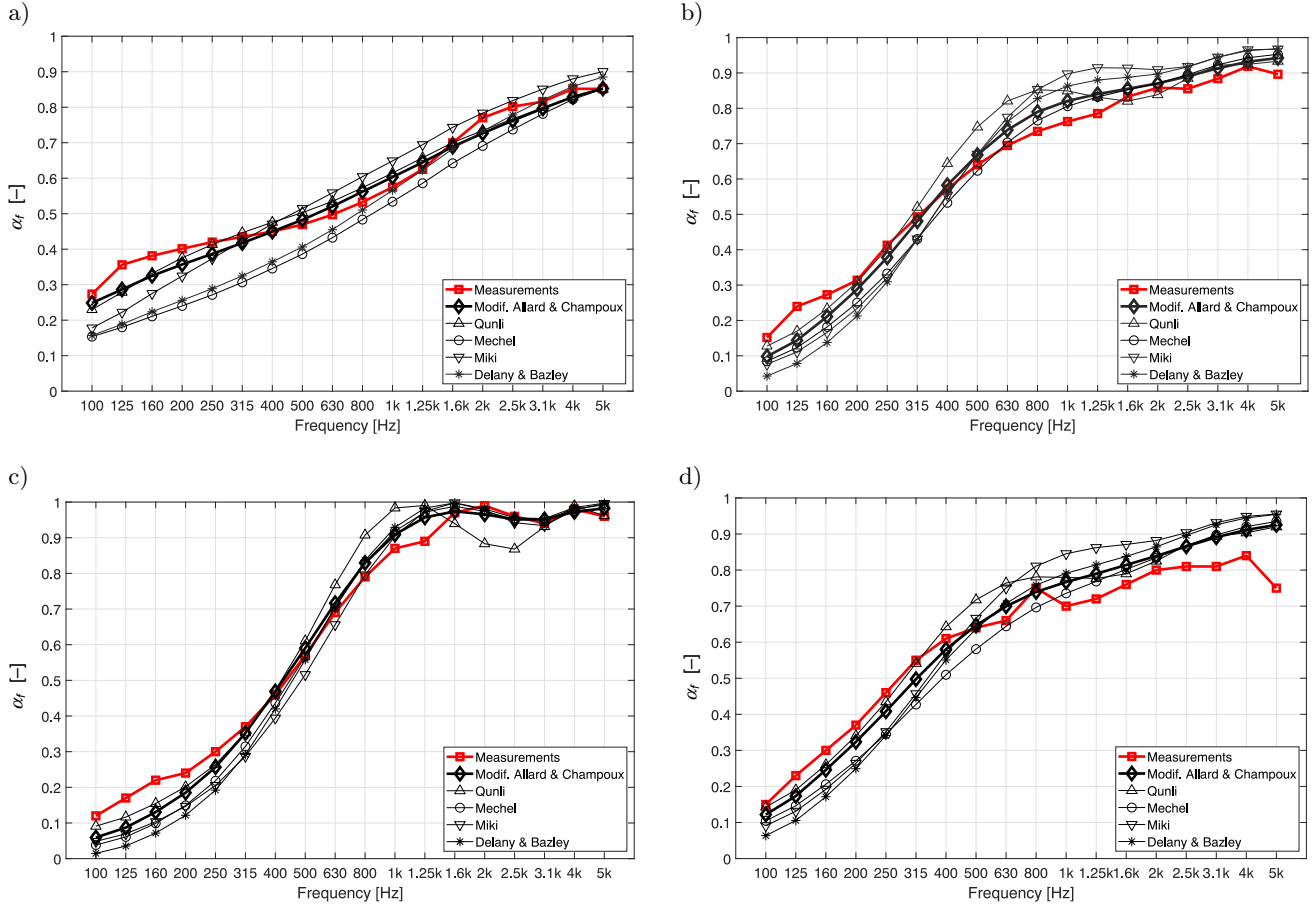


Fig. 8. Normal incidence sound absorption coefficient (α_f) determined from measurements and using empirical models for specimens: a) MW151; b) MW100; c) ME; d) PU.

tained from the measurements, root mean square errors (RMSE) were calculated for each tested material using the equation:

$$RMSE = \sqrt{\frac{\sum_{i=1}^N (x_i - \hat{x}_i)^2}{N}}, \quad (5)$$

where x_i and \hat{x}_i are the values of the measured and predicted acoustic parameter for the i -th centre frequency of the $1/3$ octave bands, respectively, and N is the total number of the centre frequencies of the $1/3$ octave bands.

The calculated values of RMSE, determining the discrepancies between α_f calculations using empirical

models and α_f obtained from measurements, are presented in Table 2.

As can be seen from Table 2, the application of the modified Allard and Champoux model brought about the best results in the form of the lowest RMSE values for all tested specimens, even though the tested materials had different structures – porous or fibrous.

5.2. Proposal of a calculation model for normal incidence sound transmission loss for mineral wools

Based on the results of the nTL of 12 material specimens in the form of mineral wool with a thickness of 20 mm, 40 mm, and 50 mm, and a density of

Table 2. RMSE for four tested materials, determining the discrepancies between α_f calculations using the empirical models and α_f obtained from measurements.

	RMSE [dB]				
	Modified Allard and Champoux	Qunli	Mechel	Miki	Delany and Bazley
MW151	0.0642	0.0648	0.0845	0.1068	0.1007
MW100	0.0432	0.0647	0.0601	0.0641	0.0755
ME	0.0327	0.0350	0.1007	0.0646	0.0863
PU	0.0442	0.062	0.055	0.086	0.086

25 kg/m³, 70 kg/m³, 110 kg/m³, and 150 kg/m³ published in (KOSALA, 2021) and, additionally, mineral wool with a thickness of 60 mm and a density of 151.4 kg/m³ (Fig. 1), it is possible to obtain a calculation model for nTL, which is a function of the frequency f and the surface density of the mineral wool specimen m_p .

The nTL spectral characteristics of the tested mineral wool can be determined using a linear function:

$$nTL = a \cdot f + b. \tag{6}$$

The dependence of the slope (a) on the surface mass (m_p) is shown in Fig. 9, however, dependence of the intercept (b) on the surface mass (m_p) is shown in Fig. 10.

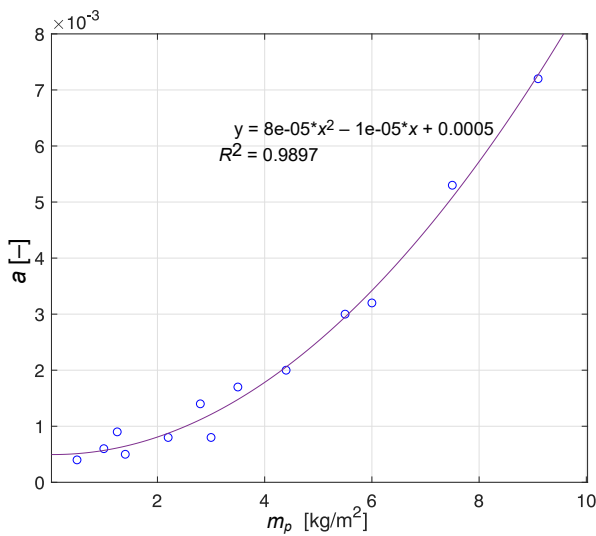


Fig. 9. Dependence of the slope (a) on the surface mass (m_p) for 13 mineral wool specimens.

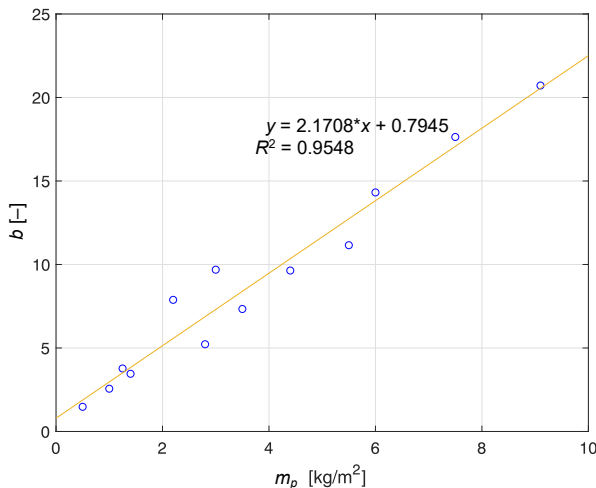


Fig. 10. Dependence of the intercept (b) on the surface mass (m_p) for 13 mineral wool specimens.

By substituting the polynomial function, shown in Fig. 9, for a and the linear function, shown in Fig. 10, for b in Eq. (6), the equation for nTL was obtained:

$$nTL = f(0.00008m_p^2 - 0.00001m_p + 0.0005) + 2.1708m_p + 0.7945 \text{ [dB]}, \tag{7}$$

where f is the frequency, and m_p is the surface density of the mineral wool.

The nTL values calculated from Eq. (7) for the 1/3 octave frequency bands in the range of 100 Hz to 5 kHz for 13 mineral wools with a density (d) from 25 kg/m³ to 151 kg/m³ and a thickness (h) from 20 mm to 60 mm are shown in Fig. 11.

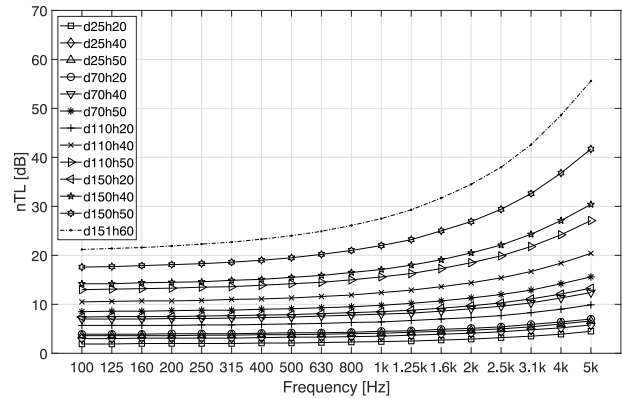


Fig. 11. Normal incidence sound transmission loss values for mineral wools with density d [kg/m³] and thickness h [mm] calculated on the basis of the surface density of the specimens.

In order to check the accuracy regarding the extent to which the nTL calculations using Eq. (7) differ from the results of experimental tests of this parameter carried out in a previous study (KOSALA, 2022) for 12 mineral wool specimens and in this work (the mineral wool MW151, corresponding to the designation d151h60 in Fig. 11), RMSE was calculated using Eq. (5). Calculations of nTL using the proposed Eq. (7) resulted in small discrepancies for the majority of mineral wool specimens compared to nTL results obtained from measurements carried out in the impedance tube. As shown in Fig. 12, RMSE \cong 1–2 dB.

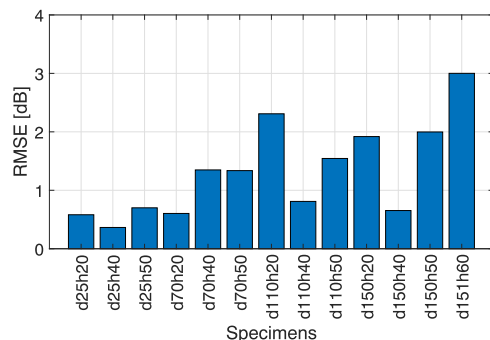


Fig. 12. RMSE for nTL calculations in relation to the values measured for thirteen mineral wool specimens.

The exception was the specimen with the highest density and thickness (d151h60), for which RMSE was equal to 3 dB.

5.3. Proposal of a calculation model for IL for a cubic enclosure with walls made of porous and fibrous materials

The IL for enclosures composed of sound-absorbing and insulating walls can be calculated using a known model based on the random incidence sound absorption coefficient of the lining material (α) and the sound reduction index (R) of the entire panel (enclosure wall) (VER, BERANEK, 2006), using the equation:

$$IL = 10 \log(\alpha) + R \text{ [dB]}. \quad (8)$$

The sound reduction index (R) of the sound-absorbing and insulating baffles constituting the enclosure wall can be obtained on the basis of laboratory tests (ISO, 2021), provided that the dimensions of the baffle are adjusted to the dimensions of the measurement window of the coupled reverberation rooms. In an approximate manner, R can be determined using theoretical calculation models appropriate to the given construction and material solution of the baffle. The validation of the model (Eq. (8)) was shown in the calculations of the IL of the prototype sound-absorbing and insulating enclosure in one work (KOSALA *et al.*, 2020b).

To calculate the IL for a cubic enclosure of an omnidirectional sound source, the walls of which are single baffles made of porous or fibrous materials, a similar formula was proposed, in which the simplification in the form of the nTL of the baffle is used instead of R :

$$IL = 10 \log(\alpha) + \text{nTL} \text{ [dB]}. \quad (9)$$

In the case of the porous and fibrous materials in question, most of which can be roughly described as locally reacting materials (ALLARD, 1992; COX, D'ANTONIO, 2017), the attenuation of sound in the material is so high that it limits the lateral transmission. The propagation direction within these materials is normal to the surface, even for oblique incidence

sound, because of refraction (COX, D'ANTONIO, 2017), therefore the surface impedance is independent of the incident wave nature. Hence, in Eq. (9), a simplification was made by replacing R with nTL.

The normal incidence sound transmission loss of such materials can be determined by testing a sample in an impedance tube, as described in Subsec. 3.2, or using a calculation model for a material of infinite extent in the lateral direction, since the boundary conditions resulting from the dimensions of the enclosure wall in the case of the materials in question are less important. Such a model for calculating nTL, based on surface mass, was proposed using Eq. (7).

The random incidence sound absorption coefficient (α) is determined according to the standard (ISO, 2005) in laboratory reverberation conditions on a material specimen of 10–12 m². However, α can also be determined using the approximate relationship between this coefficient and the α'_f , as given in (EVEREST *et al.*, 2013) in the shape of a graph. This relationship can be calculated using approximation by a second-degree polynomial with the coefficient of determination equal to $R^2 = 0.9994$ from the equation:

$$\alpha = -0.97(\alpha'_f)^2 + 1.97\alpha'_f. \quad (10)$$

The normal incidence sound absorption coefficient (α_f) can be determined by measurement using an impedance tube, as described in Subsec. 3.2, or by using theoretical calculation models, as described in Subsec. 5.1.

5.3.1. Validation of the proposed model for porous and fibrous materials

The validation of the proposed model (Eq. (9)) was carried out based on the results of experimental tests of α_f and nTL, carried out for the tested material specimens with the use of an impedance tube. The test results of these parameters are presented in Subsec. 4.1. The values of the (α) coefficient were calculated on the basis of the α_f values from Eq. (10). Figures 13–16

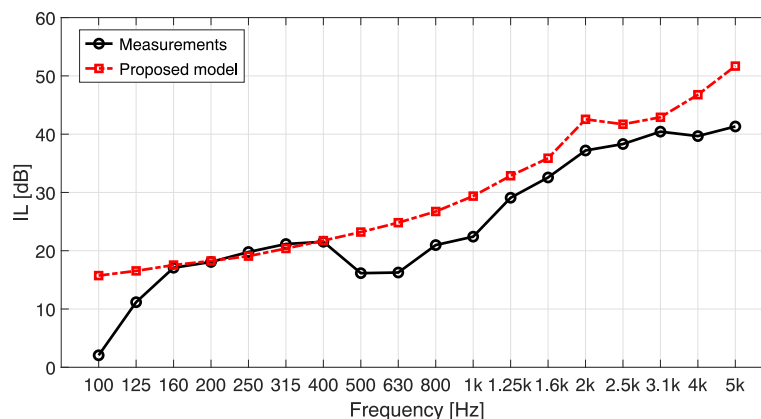


Fig. 13. Insertion loss (IL) of the enclosure made of MW151 baffles obtained from measurements and calculations using the proposed model.

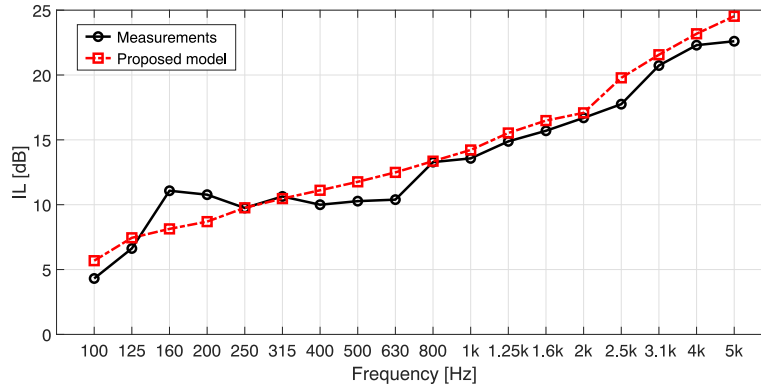


Fig. 14. Insertion loss (IL) of the enclosure made of MW100 baffles obtained from measurements and calculations using the proposed model.

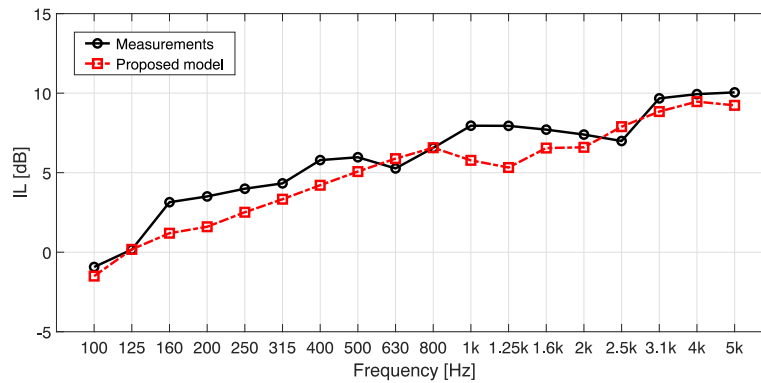


Fig. 15. Insertion loss (IL) of the enclosure made of ME baffles obtained from measurements and calculations using the proposed model.

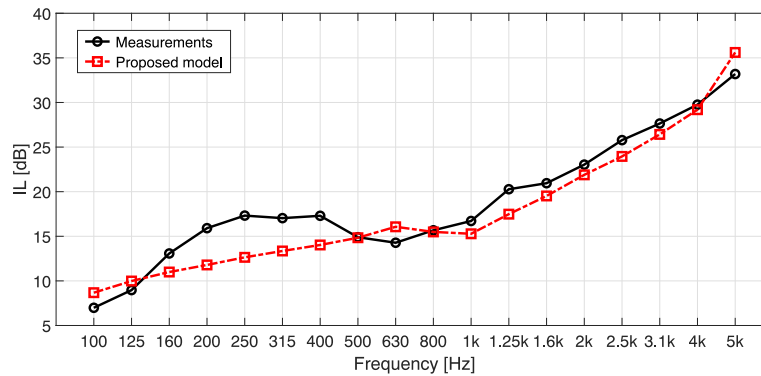


Fig. 16. Insertion loss (IL) of the enclosure made of PU baffles obtained from measurements and calculations using the proposed model.

show the IL values of enclosures with walls made of MW151, MW100, ME, and PU baffles, obtained from measurements and using the proposed IL calculation model, defined by Eq. (9).

Table 3 shows the calculated values of Pearson’s linear correlation coefficient (PCC) and RMSE, which were used to estimate the discrepancies of the results obtained from the IL calculations for the four tested materials using the proposed model (Eq. (9)) and those obtained from measurements.

For all tested materials, there is a very strong linear correlation between the results obtained from the pro-

Table 3. PCC and RMSE for four tested materials, determining the discrepancies between IL calculations using the proposed model and IL obtained from measurements.

	PCC	RMSE [dB]
MW151	0.9392	6.01
MW100	0.9734	1.38
ME	0.9551	1.30
PU	0.9581	2.34

posed model and those obtained from measurements. For the MW151 specimen, the highest RMSE value

was obtained among all specimens, which was mainly due to large discrepancies at the lowest ($f = 100$ Hz) and highest centre frequencies of the $1/3$ octave bands ($f = 5$ kHz).

5.3.2. Validation of the proposed model for mineral wool specimens

Due to the wider scope of research on the acoustic properties of mineral wool materials (KOSALA, 2021), compared to porous materials, it is possible to calculate IL, defined by Eq. (9), without the need to use an impedance tube. The knowledge of the material data is sufficient to estimate the input parameters for calculating IL, i.e., α and nTL.

The first needed parameter α is calculated on the basis of α_f from Eq. (10), while α_f can be determined using one of the known calculation models when the r value of mineral wool of a given thickness is available. For this purpose, it is proposed to use the model developed by Allard and Champoux, modified

by OLIVA and HONGISTO (2013) into an empirical model, which is much easier to use than the original semi-phenomenological model, because there is no need to determine the necessary properties of microscopic material. The second parameter, nTL, can be determined from the m_p of the mineral wool plate constituting the wall of the enclosure, using Eq. (7), as proposed in Subsec. 5.2.

The validation of the proposed model of IL (Eq. (7)) for enclosures with walls made of mineral wool plates, based on material data, was carried out using MW151 with the dimensions of $0.55 \text{ m} \times 0.55 \text{ m} \times 0.06 \text{ m}$ and MW100 with dimensions of $0.7 \text{ m} \times 0.7 \text{ m} \times 0.05 \text{ m}$. The IL values calculated and obtained from measurements in $1/3$ octave frequency bands are shown in Figs. 17 and 18.

Table 4 shows a comparison of the application of the proposed calculation model of IL, which was verified for fibrous materials in the form of MW151 and MW100 for two cases. The first concerned the use of

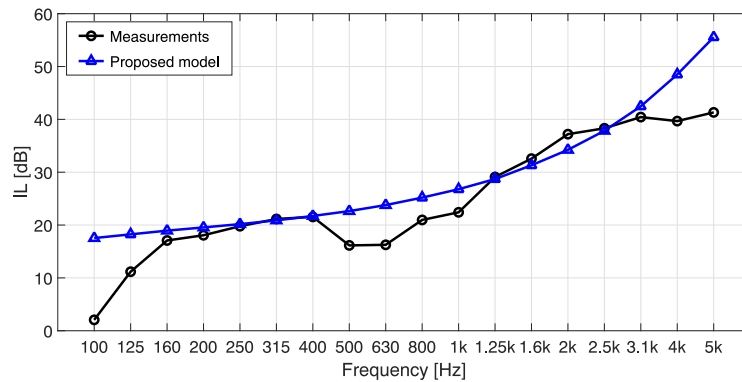


Fig. 17. Insertion loss (IL) of the enclosure made of MW151 (wall size $0.55 \text{ m} \times 0.55 \text{ m} \times 0.06 \text{ m}$) determined from measurements and calculations using the proposed model based on material data.

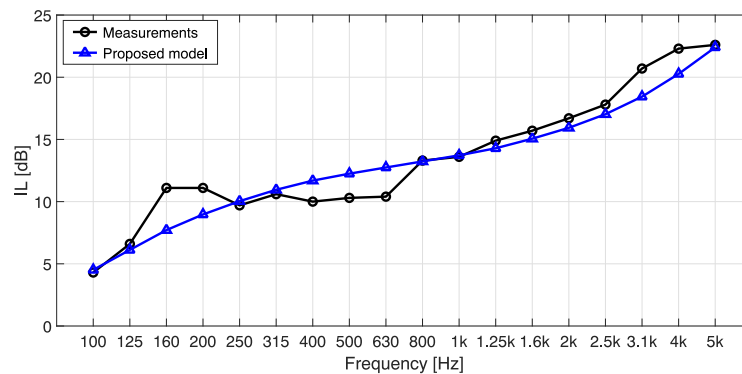


Fig. 18. Insertion loss (IL) of the enclosure made of MW100 (wall size $0.7 \text{ m} \times 0.7 \text{ m} \times 0.05 \text{ m}$) determined from measurements and calculations using the proposed model based on material data.

Table 4. PCC and RMSE for enclosures with walls made of mineral wools, determining discrepancies between IL calculated and measured for α_f and nTL obtained with the use of an impedance tube and calculation models.

	Method of determining α_f and nTL			
	Impedance tube		Calculation models	
	PCC	RMSE [dB]	PCC	RMSE [dB]
MW151	0.9392	6.01	0.8918	6.35
MW100	0.9734	1.38	0.9574	1.49

an impedance tube to determine α_f and nTL of the tested mineral wools. In the second case, α_f and nTL were obtained using the calculation models, the Allard and Champoux, and those proposed by Eq. (7), respectively.

As shown in Table 4, in the case of MW151, the IL discrepancies in the form of RMSE obtained using the calculation models for α_f and nTL are about 6.3 dB and are similar to the case when these parameters were obtained from the impedance tube. For MW100, the obtained linear correlation coefficients have similarly high values for both cases. For the two analysed methods of determining α_f and nTL needed for IL calculations, the discrepancies in the form of RMSE are similar and relatively low (around 1.5 dB).

6. Conclusions

As part of the research, two developed stands were used to enable the construction of cubic enclosures made of walls of the tested materials, intended for determining the acoustic efficiency from the penetration of sounds coming from a source placed inside. The measure of acoustic efficiency was the IL of the enclosure. The research has shown that it is possible, based on known empirical models for the sound absorption coefficient, the airflow resistance and the thickness of material specimens, to calculate the IL of an enclosure with walls made of a fibrous material, such as mineral wool. In the case of materials with a different structure, such as porous ones, for example polyurethane foam, to calculate the IL using the proposed model, it is necessary to use an impedance tube to determine the input data. This data is in the form of the α_f and the normal incidence transmission loss of the material. The results of calculations of the spectral characteristics of the IL, satisfactory for engineering purposes, were obtained for the four tested materials. The study also showed that among the empirical models such as Delany and Bazley, Miki, Mechel, Qunli, and Allard and Champoux, the latter model yielded the best results in calculating the α_f for mineral wools, melamine foam and rebonded polyurethane foam, in the form of the smallest discrepancies obtained compared to the results obtained from laboratory tests.

The second proposed calculation model for the nTL, using the surface density of a mineral wool specimen, can be used not only for calculations of the IL of the enclosure, but also for the initial estimation of nTL for mineral wools, without the use of an impedance tube. The results of the experimental and model tests obtained as part of the article in the form of acoustic parameters determining the acoustic properties of single porous and fibrous materials can also be used in further research on the modelling of layered baffles.

Acknowledgments

This research was funded by a research subvention supported by the Polish Ministry of Science and Higher Education (grant no. 16.16.130.942).

References

1. ALLARD J.F., CHAMPOUX Y. (1992), New empirical equations for sound propagation in rigid frame fibrous materials, *The Journal of the Acoustical Society of America*, **91**(6): 3346–3353, doi: [10.1121/1.402824](https://doi.org/10.1121/1.402824).
2. ASTM E2611-19 (2019), *Normal Incidence Determination of Porous Material Acoustical Properties Based on the Transfer Matrix Method*, ASTM International.
3. BATKO W., PAWLIK P., WSZOLEK G. (2017), Sensitivity analysis of the estimation of the single-number sound absorption evaluation index $DL\alpha$, *Archives of Acoustics*, **42**(4): 689–696, doi: [10.1515/aoa-2017-0071](https://doi.org/10.1515/aoa-2017-0071).
4. BERARDI U., IANNACE G. (2015), Acoustic characterization of natural fibers for sound absorption applications, *Building and Environment*, **94**(2): 840–852, doi: [10.1016/j.buildenv.2015.05.029](https://doi.org/10.1016/j.buildenv.2015.05.029).
5. BIES D.A., HANSEN C.H. (2009), *Engineering Noise Control. Theory and Practice*, 4th ed., p. 675, CRC Press Taylor & Francis Group.
6. COX T.J., D'ANTONIO P. (2017), *Acoustic Absorbers and Diffusers. Theory, Design and Application*, 3rd ed., CRC Press Taylor & Francis Group.
7. DAVY J.L. (2009), Predicting the sound transmission loss of cavity walls, [in:] *Proceedings of Interior Noise Climates: National Conference of the Australian Acoustical Society*, p. 1–16, Perth.
8. DELANY M.E., BAZLEY E.N. (1970), Acoustical properties of fibrous absorbent materials, *Applied Acoustics*, **3**(2): 105–116, doi: [10.1016/0003-682X\(70\)90031-9](https://doi.org/10.1016/0003-682X(70)90031-9).
9. ENGEL Z., SIKORA J. (1997), *Sound-Absorbing and Insulating Enclosures. The Basics of Design and Application* [in Polish: *Obudowy Dźwiękochłonna-Izolacyjne. Podstawy Projektowania i Stosowania*], Wydawnictwa AGH, Kraków.
10. EVEREST F.A., POHLMANN K.C., KURYLAK W. (2013), *Acoustic Handbook* [in Polish: *Podręcznik Akustyki*], Wydawnictwo Sonia Draga, Katowice.
11. FIEBIG W., DĄBROWSKI D. (2020), Use of acoustic camera for noise sources localization and noise reduction in the industrial plant, *Archives of Acoustics*, **45**(1): 111–117, doi: [10.24425/aoa.2020.132487](https://doi.org/10.24425/aoa.2020.132487).
12. International Organization for Standardization (2001), *Acoustics, Determination of sound absorption coefficient and impedance in impedance tubes. Part 2 Transfer-function method*, (ISO Standard No. ISO 11534-2).
13. International Organization for Standardization (2005), *Acoustics. Measurements of sound absorption in a reverberation room* (ISO Standard No. 354).

14. International Organization for Standardization (2009), *Acoustics, Determination of sound insulation performances of enclosures. Part 1: Measurements under laboratory condition (for declaration purposes)* (ISO Standard No. ISO 11546-1).
15. International Organization for Standardization (2010), *Acoustics, Determination of sound power levels and sound energy levels of noise sources using sound pressure, Survey method using an enveloping measurement surface over a reflecting plane* (ISO Standard No. 3746).
16. International Organization for Standardization (2020), *Acoustics, Determination of the airflow resistance, Part 2: Alternating airflow method* (ISO Standard No. ISO 9053-2), <https://www.iso.org/standard/76744.html>.
17. International Organization for Standardization (2021), *Acoustics, Laboratory measurement of sound insulation of building elements. Part 2: Measurement of airborne sound insulation* (ISO Standard No. ISO 10140-2), <https://www.iso.org/standard/79487.html>.
18. JIANG Y., CHEN S., WANG D., CHEN J. (2017), Multi-objective optimization of acoustical properties of PU-bamboo-chips foam composites, *Archives of Acoustics*, **42**(4): 707–714, doi: [10.1515/aoa-2017-0073](https://doi.org/10.1515/aoa-2017-0073).
19. KOSALA K. (2021), Experimental tests of the acoustic properties of sound-absorbing lining and cores of layered baffles, *Vibrations in Physical Systems*, **32**(1): 2021107, doi: [10.21008/j.0860-6897.2021.1.07](https://doi.org/10.21008/j.0860-6897.2021.1.07).
20. KOSALA K. (2022), Experimental tests and prediction of insertion loss for cubical sound insulating enclosures with single homogeneous walls, *Applied Acoustics*, **197**: 108956, doi: [10.1016/j.apacoust.2022.108956](https://doi.org/10.1016/j.apacoust.2022.108956).
21. KOSALA K., MAJKUT L., MLECZKO D., OLSZEWSKI R., WSZOŁEK T. (2020a), Accuracy of prediction methods for sound insulation of homogeneous single baffles, *Vibration in Physical Systems*, **31**(2): 2020210, doi: [10.21008/j.0860-6897.2020.2.10](https://doi.org/10.21008/j.0860-6897.2020.2.10).
22. KOSALA K., MAJKUT L., OLSZEWSKI R. (2020b), Experimental study and prediction of insertion loss of acoustical enclosures, *Vibrations in Physical Systems*, **31**(2): 2020209, doi: [10.21008/j.0860-6897.2020.2.09](https://doi.org/10.21008/j.0860-6897.2020.2.09).
23. KUNIO J., YOO T., JOU K., BOLTON J.S., ENOK J. (2009), A comparison of two and four microphone standing wave tube procedures for estimating the normal incidence absorption coefficient, [in:] *Proceedings of 38th International Congress and Exposition on Noise Control Engineering*, pp. 1057–1065.
24. MECHEL F.P. (1988), Design charts for sound absorber layers, *The Journal of the Acoustical Society of America*, **83**(3): 1002–1013, doi: [10.1121/1.396045](https://doi.org/10.1121/1.396045).
25. MIKI Y. (1990), Acoustical properties of porous materials – modifications of Delany–Bazley models, *Journal of the Acoustical Society of Japan (E)*, **11**(1): 19–24, doi: [10.1250/ast.11.19](https://doi.org/10.1250/ast.11.19).
26. MORZYŃSKI L., SZCZEPAŃSKI G. (2018), Double panel structure for active control of noise transmission, *Archives of Acoustics*, **43**(4): 689–696, doi: [10.24425/aoa.2018.125162](https://doi.org/10.24425/aoa.2018.125162).
27. NIERADKA P., DOBRUCKI A. (2018), Insertion loss of enclosures with lined slits, [in:] *Proceedings of 11th Euronoise 2018*, pp. 893–898.
28. NURZYŃSKI J. (2022), Sound insulation of lightweight external frame walls and the acoustic effect of additional thermal insulation, *Applied Acoustics*, **190**(15): 08645, doi: [10.1016/j.apacoust.2022.108645](https://doi.org/10.1016/j.apacoust.2022.108645).
29. OLIVA D., HONGISTO V. (2013), Sound absorption of porous materials – Accuracy of prediction methods, *Applied Acoustics*, **74**(12): 1473–1479, doi: [10.1016/j.apacoust.2013.06.004](https://doi.org/10.1016/j.apacoust.2013.06.004).
30. PUTRA A., KHAIR F.A., NOR M.J.M. (2015), Utilizing hollow-structured bamboo as natural sound absorber, *Archives of Acoustics*, **40**(4): 601–608, doi: [10.1515/aoa-2015-0060](https://doi.org/10.1515/aoa-2015-0060).
31. QUNLI W. (1988), Empirical relations between acoustical properties and flow resistivity of porous plastic open-cell foam, *Applied Acoustics*, **25**(3): 141–148, doi: [10.1016/0003-682X\(88\)90090-4](https://doi.org/10.1016/0003-682X(88)90090-4).
32. SHARP B.H. (1973), *A study of techniques to increase the sound installation of building elements*, US Department of Commerce, National Technical Information Service.
33. TRINH V.H., NGUYEN T.V., NGUYEN T.H.N., NGUYEN M.T. (2022), Design of sound absorbers based on open-cell foams via microstructure-based modeling, *Archives of Acoustics*, **47**(4): 501–512, doi: [10.24425/aoa.2022.142894](https://doi.org/10.24425/aoa.2022.142894).
34. VER I.L., BERANEK L.L. (2006), *Noise and Vibration Control Engineering: Principles and Applications*, John Wiley & Sons, Inc., Hoboken, New Jersey.